Available online at www.sciencedirect.com

ScienceDirect

Scripta Materialia 83 (2014) 9–12

Scripta MATERIALIA

www.elsevier.com/locate/scriptamat

A fast grain-growth mechanism revealed in nanocrystalline ceramic oxides

Dilpuneet S. Aidhy,[a,*] Yanwen Zhang[a,b] and William J. Weber[a,b]

[a] *Materials Science and Technology Division, Oak Ridge National Laboratory, Oak Ridge, TN 37831, USA*
[b] *Materials Science and Engineering, University of Tennessee, Knoxville, TN 37996, USA*

Received 7 February 2014; revised 6 March 2014; accepted 24 March 2014
Available online 1 April 2014

Grain growth issues in nanocrystalline ceramic oxides render their highly attractive properties practically unusable due to limited understanding of the underlying grain-growth mechanisms. Two conventional "slow" grain-growth mechanisms, i.e. curvature driven and grain-rotation driven, are shown to be thermally active, and the discovery of a "fast" disorder-driven mechanism is revealed using molecular dynamics simulation on nanocrystalline ceria, in conjunction with experimental observations. We show that this disorder mechanism drives the unexpected fast grain growth observed experimentally during synthesis and irradiation conditions.

Keywords: CeO_2; Nanocrystalline ceramic oxide; Grain growth; Molecular dynamics simulation; Radiation damage

Grain growth is a well-observed microstructural evolution feature that has been widely studied for decades [1–3]. The conventional picture of grain growth is that it is a thermally activated phenomenon that follows the curvature-driven grain boundary (GB) mechanism. In addition, grain growth can also occur via a grain-rotation mechanism, primarily in nanocrystalline materials [1–8]. Experimental studies on nanocrystalline ceria and zirconia, two typical ceramic oxides that are highly attractive and widely applicable engineering materials for electronics [9], energy [10–12] and biomedical applications [13], show thermal grain growth at temperatures well above 873 K [14] and 1125 K [15], respectively. However, an unusual and rapid grain growth has been recently observed at temperatures as low as 160 K, where nanograins ~6–8 nm in size grew to ~25 nm in nanocrystalline ceria [16] and zirconia [17] under ion irradiation. Interestingly, similar signatures of rapid grain growth (with very low GB activation energies) have been frequently reported [14,18–25] during the synthesis of nanocrystalline materials from such different techniques as spray pyrolysis, pulsed laser deposition and sintering, showing significant deviation from the normal/slower rates of grain growth generally observed in microcrystalline materials. Thus this rapid grain growth appears to be a unique feature to nanocrystalline materials that does not seem to follow the conventional grain-growth laws.

Figure 1 illustrates the irradiation–induced grain growth in nanocrystalline ceria under 3 MeV Au^+ ions from 0.3 dpa. Comparison of the as-deposited and irradiated structures at 300 K in Figure 1a and b respectively reveals the growth of grains due to irradiation, while Figure 1c illustrates the average grain growth. The grain growth occurs very rapidly in the smaller grains, and the change in the slope of the curve indicates the operation of two different mechanisms. Similarly, during synthesis of nanocrystalline ceria, rapid initial grain growth with an activation energy of 0.7 eV compared to 5 eV in polycrystalline counterpart is observed (see Fig. 1d, reproduced from Ref. [26]), again revealing the operation of a different, faster grain-growth mechanism. Therefore, there appears to be an unknown, unique grain-growth-driving mechanism in nanocrystalline ceramic oxides common to the synthesis and irradiation conditions, and responsible for the unexpected rapid grain growth behavior. In this work, using nanocrystalline ceria as a model system, we report the discovery of a new disorder-driven mechanism, where the loss of

* Corresponding author. Address: One Bethel Valley, PO Box 2008, MS 6138, Oak Ridge, TN 37831, USA. Tel.: +1 865 241 2720; e-mail: aidhyds@ornl.gov

http://dx.doi.org/10.1016/j.scriptamat.2014.03.020
1359-6462/

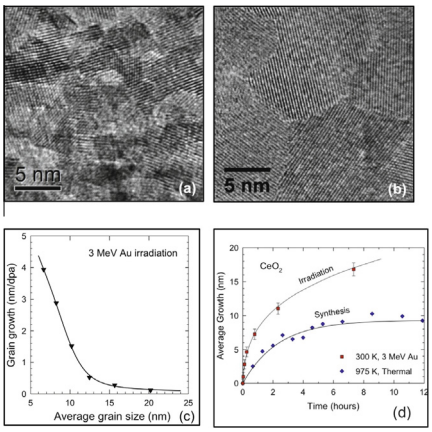

Figure 1. (a) As-deposited nanocrystalline ceria. (b) Irradiation-induced grain growth due to 3 MeV Au^{+} at 300 K. (c) Faster gain growth in the smaller grains compared to larger grains as shown by the change in slope of the curve illustrating the operation of two different grain-growth mechanisms. (d) Grain growth in ceria under two different conditions: (1) irradiation and (2) spray-pyrolysis synthesis. Grain growth under both conditions occurs rapidly compared to normal microcrystalline thermal grain growth (not shown), revealing that the grain growth processes in nanocrystalline materials occur at a much faster rate than in microcrystalline counterparts. The synthesis curve is reproduced from Ref. [26].

crystalline order is the key leading to grain growth in nanocrystalline materials. We reveal that this disorder mechanism drives the unexpectedly fast grain growth observed experimentally under both synthesis and cryogenic ion-irradiation conditions. This new understanding of the grain-growth mechanism could serve as a viable route to controlling nanograin sizes in the design and tailoring of oxide materials, particularly for energy applications [27].

Molecular dynamics (MD) simulations have been instrumental in unraveling various microstructural evolution mechanisms [5,28–30]. In particular, these simulations have revealed the grain-rotation-driven grain-growth mechanism in metals [5]. Here we use these simulations to capture, for the first time, thermal grain growth in ceramic oxides via the two conventional mechanisms, then demonstrate the prevalence of the third mechanism. To capture GB movement on the limited MD timescale, simulations are performed at high temperatures, i.e. above 2000 K. We model nanocrystalline ceria using a point-ion classical interatomic potential developed by Gotte et al. [31], where the short-range interactions are described by a rigid-ion Buckingham-type potential. This potential has previously shown to accurately predict point-ion dynamics; the details on its fidelity can be found elsewhere [32,33]. The long-range coulombic interactions are evaluated via Wolf's direct $1/r$ coulombic summation method [34], with spherical truncation at the cut-off radius of 10.71 Å. The zero-temperature lattice parameter thus obtained is the experimental value of $a_0 = 5.411$ Å to which it was fitted [31]. We use the Voronoi tessellation method [35] to construct [1 0 0] columnar structures within the three-dimensional cell containing grains of different number of sides shapes and fill the grains by placing ions on a rotated fluorite lattice of CeO_2. In the grain boundary regions, an ion is removed if it is closer to a neighboring ion by 1.5 Å while maintaining charge neutrality. For all our structures, we ensure that the misorientation angles between the two grains are larger than or equal to 30° to create high-angle grain boundaries. The initial $T = 0$ K structures are out of equilibrium; they are therefore equilibrated by gradually raising the temperature to the desired simulation temperatures to relax the grain boundaries. This is a typical method that has been widely used previously to create nanocrystalline structures for MD simulations [28,36].

We first capture grain growth via the two conventional mechanisms. We use a six-grained nanostructure of dimensions $16a_0 \times 10a_0 \times 9a_0$, with each grain of diameter ~3 nm containing 16,497 ions in total. A snapshot of the structure equilibrated to 2000 K at 700 ps is shown in Figure 2a. The misorientation between the two grains is shown by the black line. Progressive snapshots of the evolving microstructure at $t = 2670$, 3660 and 3755 ps are shown in Figure 2b–d, respectively. The microstructure first evolves by the grain-rotation mechanism. Figure 2b shows that grains 1 and 4 rotate anticlockwise and clockwise, respectively, and their misorientation angle decreases over time. In Figure 2c, the misorientation between them is completely annihilated and the GB has disappeared, resulting in grain coalescence. This simulation hence captures grain rotation in ceramic oxides and illustrates grain growth.

Beyond this stage, the microstructure shows a transition from the grain-rotation mechanism to the curvature-driven grain boundary movement mechanism. This is illustrated by grain boundaries labeled "a" in Figure 2c and "b" in Figure 2d that gradually move towards the center of grain 2, leading to the disappearance of grain 2 in Figure 2d and thus illustrating the grain growth via a curvature-driven mechanism. With time, eventually all the GBs will be annihilated, and the structure will evolve into a single crystal. Figure 2e

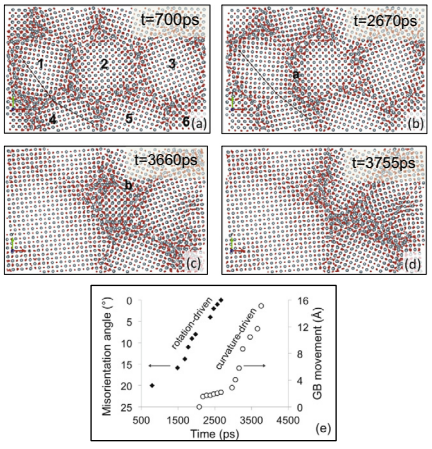

Figure 2. The grain-rotation and curvature-driven grain-growth mechanisms. (a, b) Rotation of grains 1 and 4, leading to elimination of the grain boundary between them. (c, d) Shrinkage of grain 2 due to movement of the grain boundaries labeled "a" and "b" by the curvature-driven mechanism. (e) Grain rotation and GB movement via the curvature-driven mechanism vs. time. The former occurs over ~2500 ps, the latter over ~800 ps. The black lines in (a) and (b) are guides for the eye to show grain orientation.

shows the degree of grain rotation and the GB movement by the curvature-driven mechanism as functions of time. The grain rotation takes ~2500 ps to annihilate this specific misorientation, and the GB "a" movement by the curvature-driven mechanism takes ~800 ps before grain 2 fully disappears.

Interestingly, this simulation shows that, while the two mechanisms are operational, the grains maintain their crystallinity. Even when grain 2 in Figure 2c shrinks to a size of less than 1 nm, it still maintains the fluorite crystal structure. We later show that the third mechanism is exactly the opposite of these two, and it only becomes active when the grains are highly disordered.

Having demonstrated the two conventional mechanisms of grain growth, we now show the third mechanism using a seven-grain $16a_0 \times 16a_0 \times 9a_0$ structure containing 27,576 ions, as shown in Figure 3. A snapshot of the 2000 K equilibrated structure at $t = 958$ ps is shown in Figure 3a. The snapshots at $t = 998$, 1037 and 1285 ps are shown in Figure 3b–d, respectively. We focus on grain 5, which is initially crystalline. At times between Figure 3a and Figure 3b (not shown), it is observed that the disorder originates from the triple junction between grains 5, 6 and 7, and eventually consumes grain 5. This disorder persists for ~100 ps, after which the disordered volume is consumed by the epitaxial growth of grain 6 into grain 5. We see that, in this simulation, the microstructure evolves by neither of the two conventional mechanisms; rather, it evolves by disordering of the grain. What is also interesting to note is that the grain growth occurs on a very short timescale compared to the other two mechanisms. We will discuss this fast kinetics of this disorder mechanism later in this letter. A movie illustrating the complete evolution via this disorder mechanism is presented in the Supplemental Information section.

We now connect this prediction from computer simulations to the experimental observations. We recall the unexpected fast grain growth previously observed experimentally under thermally annealing [18,20,22] and under irradiation conditions [16,17]. Atomic disordering is well known to occur during the synthesis of nanocrystalline films and under irradiation conditions; therefore, it is very likely that the experimentally observed fast grain growth also occurs by this disorder-driven mechanism. In addition, we recently demonstrated that irradiation-induced grain growth in nanocrystalline ceria and zirconia is dependent on the total energy deposition from both ionization and collision processes [37], and both processes contribute to defect production and lattice disordering [38,39]. Here, we demonstrate how the introduction of such atomic disorder leads to grain growth in the absence of the two conventional mechanisms.

We employ a nine-grain $61a_0 \times 39a_0 \times 9a_0$ structure containing 245,565 ions equilibrated at 2300 K, as shown in Figure 4. We artificially disorder the nine-grain structure by randomly displacing 35% Ce ions from their lattice sites by at least 1 Å and up to 1 a_0 in one grain, as shown in Figure 4a. It should be pointed out that such high levels of cation disorder (up to 60%) are readily attained in single-crystal ZrO_2 [40] and UO_2 [41] under ion irradiation. We do not directly disorder the oxygen sublattice because it has been shown previously in fluorite-structured oxides that defects on the cation sublattice are primarily responsible for damage and will induce disorder on the oxygen sublattice whereas, in the absence of cation defects, oxygen defects are unstable and recover [33,42]. This cation-induced disordering is exactly what is shown in the snapshot

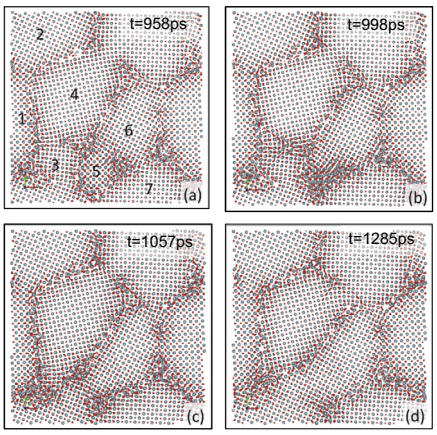

Figure 3. The grain-disorder-driven grain-growth mechanism. Grain 6 grows by consuming grain 5 in two steps. First, grain 5 becomes disordered by completely losing its crystallinity in (b) and (c). It then recovers by regaining its crystallinity, but only in the same orientation as that of the neighboring grain 6, leading to the growth of grain 6 in (d).

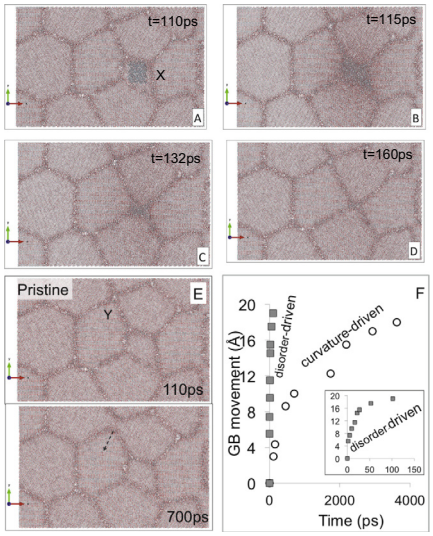

Figure 4. (a–d) Irradiated (disordered) grain growth. Disorder in a grain leading to disappearance of the damaged grain, and growth of the neighboring grains. (a) A $T = 2300$ K equilibrated nine-grained nanocrystalline structure at $t = 110$ ps with a disordered Ce lattice. Equilibration at (b) $t = 115$ ps, (c) $t = 132$ ps and (d) $t = 160$ ps. The disorder created in (a) quickly consumes the whole grain, leading to its rapid disappearance. All four neighboring grains concomitantly grow at its expense. (f) Similar $T = 2300$ K equilibration of the structure without the initially added disorder. The GB marked Y barely moves in 700 ps. (f) Time comparison of the GB movement revealing only ~50 ps is required for the GB marked X to move by 18 Å, compared to ~3700 ps by GB Y via the curvature-driven mechanism, illustrating that the disorder mechanism works on a much faster time scale compared to the conventional mechanism.

taken at $t = 115$ ps in Figure 4b, where the oxygen sublattice becomes disordered. We see that, once the disordered structure is equilibrated, the disorder spreads throughout the grain. With time, the disordered volume is consumed by the neighboring grains, as shown by the snapshots at 115 and 132 ps in Figure 4b and c, respectively, and by $t = 160$ ps in Figure 4d the grain has completely disappeared.

Interestingly, the grain growth occurs very rapidly. Not only has the disorder disappeared by 160 ps, but the grains have also grown within these 50 ps. In contrast, the other two mechanisms of grain growth occur at a much slower rate. We compare the time evolution of the disordered-grain structure to a pristine structure in Figure 4e and f, starting with identical structures at 110 ps. While, in the disordered case, the grain disappears and the other grains grow by 160 ps, demonstrating rapid microstructural evolution, the pristine structure shows minimal evolution at times of up to 700 ps in Figure 4e. In fact, we find that it takes the order of a few nanoseconds for either of the two conventional mechanisms to become active. In contrast to ~3700 ps for the GB (marked Y in Fig. 4e) to move by 18 Å via the curvature-driven mechanism, it takes only 50 ps for the GB marked X to move by the same distance via the disorder-driven mechanism, thus revealing the rapidity of the mechanism, as shown in Figure 4f. A magnified view of the disorder-driven rate is shown in the inset. We believe that this is the critical difference that sets the disorder-driven mechanism apart from the other two, and is the key reason for the rapid grain growth observed experimentally.

Finally, we observe that the amount of disorder may dictate whether the disorder mechanism dominates grain growth. We compared two structures (not shown), one with 75% disorder and the other with 15%, but with identical initial structures. While we use this unusually large amount of disorder to illustrate the concept via time-limited MD simulations, there are instances where disorder up to 50% has been experimentally observed in similar materials (e.g. ZrO_2) previously [40,41,43]. Due to the very high disorder that spreads throughout the grain, the former structure (and the grain) followed the disorder mechanism, leading to a very rapid grain growth process. In contrast, the latter structure evaded the disorder mechanism. The smaller amount of initial disorder prevented the damaged grain from exceeding the barrier for grain shrinkage. Instead, the grain recovered from the disorder and annealed back to its crystalline order. The other two (slower) mechanisms then took over, and the grain growth proceeded by grain rotation. The structure eventually evolved similar to that in Figure 2.

From the radiation-damage experimental standpoint, these simulations show that there has to be a strong relationship between grain size and deposited energy density per ion (or disorder concentration) to lead to grain growth by the disorder mechanism. When the grain size is smaller than or comparable to the damage size, the large lateral damage volume created by an incident ion would result in grain growth, as also proposed by Liu et al. [44] for metals. This grain growth would, however, level off as the grain size becomes larger than the damaged volume. As shown recently [37], the incident ion damage volume is of the order of 10 nm diameter and will, at initial small grain sizes, encompass more than one grain. These simulations show that the elements of disorder must dominate those of crystallinity for grain growth to take place. What is also important to note is that irradiation is a mere agent in creating additional disorder in a system. Nanocrystalline grains will grow thermally even in the absence of irradiation, as long as there is enough local disorder in the system [45]. This is particularly true in nanocrystalline thin film ceramic oxides, where thin film fabrication is normally under conditions that limit not just grain growth, but also high crystallinity, leaving varying amounts of disorder from grain to grain. This available disorder during material synthesis is the reason why fast grain growth is observed experimentally [14,18,19]. The results of the present study suggest that reduction of disorder via irradiation (i.e. improvement in crystallinity) and limited grain growth may be possible in these technologically important nanocrystalline oxide films.

In conclusion, we reveal a grain-growth mechanism in ceramic oxides that occurs via a grain disorder mechanism on a much shorter timescale than the two conventional mechanisms. The simulations predict that this mechanism could be responsible for the fast grain growth observed experimentally under both material synthesis [14,18,19,22] and irradiation [16,17] conditions. This mechanism is also the reason why the grain growth occurs at low temperatures and provides a more controlled mechanism for improving crystallinity with limited grain growth. The unraveling of this mechanism now opens up new possibilities to better control grain sizes, improve crystallinity and tailor the functionality of nanocrystalline materials.

This work was supported as part of the Materials Science of Actinides, an Energy Frontier Research Center funded by the U.S. Department of Energy, Office of Science, Office of Basic Energy Sciences. The computer simulations were performed at the National Energy Research Scientific Computing Center at Lawrence Berkeley National Laboratory.

Rest of the references can be found in the Supplemental section.

Supplementary data associated with this article can be found, in the online version, at http://dx.doi.org/10.1016/j.scriptamat.2014.03.020.

[1] J. von Neumann, Metal Interfaces, ASM, Cleveland, OH, 1952.
[2] J.E. Burke, D. Turnbull, Prog. Metal Phys. 3 (1952) 220.
[3] W.W. Mullins, J. Appl. Phys. 27 (1956) 900.
[4] G. Gottstein, L.S. Shvindlerman, Grain Boundary Migration in Metals, CRC Press, Boca Raton, FL, 1999.
[5] A.J. Haslam, S.R. Phillpot, D. Wolf, D. Moldovan, H. Gleiter, Mater. Sci. Eng., A 318 (2001) 293.
[6] P. Feltham, Acta Metall. 5 (1957) 97.
[7] K.E. Harris, V.V. Singh, A.H. King, Acta Mater. 46 (1998) 2623.
[8] L.J. Moore, R.D. Dear, M.D. Summers, R.P. Dullens, G.A. Ritchie, Nano Lett. 10 (2010) 4266.